Mendeleev Communications

Mendeleev Commun., 2025, **35**, 148–151

Mechanisms of action of the antibiotic ciprofloxacin on the DNA-binding protein Dps detected by molecular modeling techniques

Ksenia B. Tereshkina,*[a] Eduard V. Tereshkin,[a] Vladislav V. Kovalenko,[a] Yurii F. Krupyanskii[a] and Nataliya G. Loiko[b]

[a] *N. N. Semenov Federal Research Center for Chemical Physics, Russian Academy of Sciences, 119991 Moscow, Russian Federation. E-mail: ksenia.tereshkina@chph.ras.ru*

[b] *Federal Research Center 'Fundamentals of Biotechnology' of the Russian Academy of Sciences, 119071 Moscow, Russian Federation. E-mail: loikonat@mail.ru*

DOI: 10.71267/mencom.7567

A comprehensive analysis of the effect of the antibiotic ciprofloxacin on the DNA-binding protein Dps of the bacterium *Escherichia coli* was carried out using three molecular modeling methods: docking, umbrella sampling for calculating mean force potential profiles and classical molecular dynamics. It was shown that ciprofloxacin can penetrate into the internal cavity of the protein, as well as adsorb to the surface, reducing the ability of the N-termini to bind DNA.

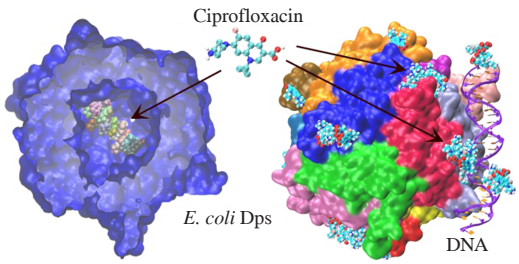

Keywords: DNA-binding protein Dps, antibiotic ciprofloxacin, docking, classical molecular dynamics, umbrella sampling, mean force potential profiles, free energy.

The DNA-binding protein Dps is an essential, universally conserved protective protein of prokaryotes, identified in the vast majority of bacterial species and some archaea.[1] It belongs to the nucleoid-associated proteins along with HU, IHF, CbpB, Fis, H-NS, CbpA and other proteins. In the logarithmic growth phase of a bacterial culture, the content of this protein in a cell is about 6000 molecules, and it increases 30-fold upon transition to the stationary growth phase of a bacterial culture. In the stationary phase, this is the most numerous nucleoid-associated protein in a bacterial cell. Dps is a homolog of ferritin, is also spherical in shape and has a cavity inside. But unlike 24-subunit ferritin, Dps is a homododecamer with a diameter of ~9 Å, with a cavity with a diameter of about 4–5 Å (Figure 1).[2] The properties and mechanisms of action of this protein have been studied best using the example of the gram-negative bacterium *Escherichia coli*.[3,4] It has been shown that the main functions of Dps are to protect cells from oxidative stress, sequester iron and preserve DNA by forming stable complexes during the stationary phase of bacterial culture growth.[5,6] The last of these functions helps prokaryotic cells not only survive prolonged starvation, but also become more resistant to any stressful effects, including the action of antimicrobial agents.[7] The presence of such a protein in pathogens *Yersinia pestis*, *Mycobacterium tuberculosis*, *Staphylococcus aureus*, *Salmonella enterica*, *etc.* is considered one of the factors that impart resistance to antibiotics.[8,9]

Although the properties, molecular mechanisms and interactions with other substances of the Dps family of proteins have been thoroughly studied over the past 30 years, many aspects remain poorly understood, including the effect of various antibiotics on the protein. This problem is due to the objective complexity of setting up experiments *in vivo* and *in vitro*. However, the development of computer technologies now makes it possible to effectively study the mechanisms of interaction of small molecules at the atomic level *in silico*. Various molecular modeling methods are successfully used to study the properties of various proteins and the mechanisms of their interaction with other substances.[10,11] Previously, using modern classical molecular dynamics methods, we were able to predict how the protective properties of the Dps protein under desiccation stress will depend on the cultivation temperature of *E. coli* bacteria.[12] We also showed the concentration dependence of the effect of a chemical analogue of the bacterial anabiosis inducer 4-hexylresorcinol on Dps and *E. coli* cells.[13] The results of molecular modeling were successfully confirmed by experimental data.

In this work, the effect of the antibiotic ciprofloxacin (Cip) on the Dps protein was investigated using molecular modeling. Three modern modeling methods were used to obtain a comprehensive picture of the interaction. To detect Cip-binding pockets on the Dps protein surface and to estimate their 'attractiveness' for the antibiotic (based on the free energy of binding), we used one of the high-throughput ligand-binding site search methods, namely docking.[14] To determine the potential for Cip to penetrate the protein globule, the umbrella sampling method was applied to compute the potential of mean force.[15] The main assessment of the molecular mechanisms of the dynamic interaction of Cip and Dps in solution was carried out using the classical molecular dynamics method, which is a capacious tool for studying the evolution of intermolecular communications at the atomic level.[16]

The antibiotic Cip, which belongs to the class of fluoroquinolones, is often used in medicine to treat a number of diseases.[17] It has been proven that its main mechanism of action is to stop DNA replication by blocking the A-subunit of DNA gyrase, as well as to affect the substances of bacterial cell walls.[18] However, other intracellular targets of this antibiotic have recently been identified, including DNA and DNA-associated

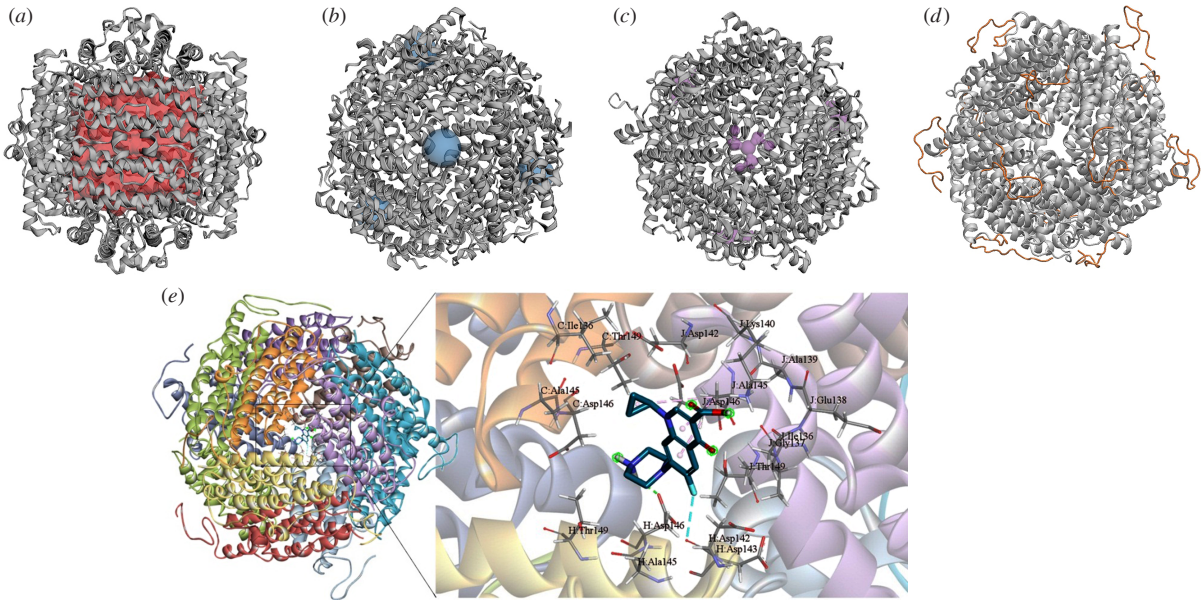

Figure 1 Possible Cip binding sites on the outer and inner surfaces of the *E. coli* Dps protein: (*a*) internal cavity (red), (*b*) ferritin pore pocket (blue), (*c*) Dps pore pocket (purple) and (*d*) protein N-termini (orange). (*e*) View from the ferritin pore side of Dps (different colors represent different protein subunits). Inset: location of the Cip molecule within the ferritin pore pocket according to the docking results.

proteins.[19,20] Therefore, studying the effect of Cip on the Dps protein is an urgent task, the solution of which is directly related to solving the problem of antibiotic resistance.

The Dps protein was modeled based on the PDB ID: 6QVX structure to which the missing N-terminal amino acid residues were added. To find possible Cip binding sites on the outer and inner surfaces of the Dps protein, a search of pockets (docking sites) was performed using CastP.[19] Cip docking over the entire protein surface was carried out using AutoDock and AutoDock Vina with the Lamarckian genetic algorithm as the scoring function in the PyRx package. Charges were assigned to the protein and ligand structures using AutoDock Vina. Since the Dps protein does not have a defined active site, rectangular boxes were used to determine the binding sites both for the entire protein molecule as a whole and for the identified pockets separately, namely: the internal cavity [Figure 1(*a*)], four ferritin pores [Figure 1(*b*)], four DPS pores [Figure 1(*c*)] and other pockets and voids in the protein structure, as well as regions near the N-termini of the protein [Figure 1(*d*)]. The positions of the centers and the sizes of the boxes were adjusted for a specific search. It turned out that in addition to the internal cavity with a volume of $V \approx 38$ nm^3, pockets can be identified on the protein surface in ferritin pores ($V \approx 0.25$ nm^3), between two neighboring subunits ($V \approx 0.05$ nm^3), in the Dps pores ($V \approx 0.02$ nm^3) and a number of small pockets along the entire outer surface. The binding affinity (free energy, ΔG) of Cip and Dps was estimated taking into account the distance (L) between the centers of mass of the protein and Cip. Cip docking studies revealed that the antibiotic has an average binding affinity to the ferritin pores of Dps ($\Delta G = -6.925 \pm 0.250$ kcal mol^{-1}, $L \approx 3.6$ nm), to a lesser extent to the areas of the internal cavity near the Dps pores ($\Delta G = -6.675 \pm 0.096$ kcal mol^{-1}, $L \approx 2$ nm) and the N-termini of the protein ($\Delta G = -6.701 \pm 0.070$ kcal mol^{-1}, $L \approx 4.6$ nm). With low binding affinity, Cip binds inside the protein cavity to two or three neighboring subunits ($\Delta G \geqslant -5.7$ kcal mol^{-1}). Thus, the most biologically interesting binding sites for Cip are the ferritin pores [see Figure 1(*b*)], the internal cavity [see Figure 1(*a*)] and the N-termini of the protein [see Figure 1(*d*)]. The pockets of the ferritin pores are spatially connected with the internal cavity and can presumably serve as a pathway for Cip migration into the protein. Inside the ferritin pore, the Cip molecule is coordinated by three protein subunits (see Figure 1). The relative sizes of the pore and Cip suggest possible penetration of the antibiotic into the protein. Moreover, according to docking data, the energetically most favorable binding sites inside the protein cavity are the amino acid residues Glu64 near the Dps pores from the internal cavity side of the protein.

To test the hypothesis of Cip penetration into the protein, we considered complexes of Dps with Cip obtained as a result of docking inside the ferritin pore. Using the method of steered molecular dynamics, a force was applied to the Cip molecule, pushing the molecule along the axis passing through the ferritin pore, the opposite pore of Dps and the center of mass of the protein. A straight line was chosen based on the considerations that the ferritin pores lie opposite the pores of Dps, *i.e.*, it is possible that small molecules migrate directly from the solution, through the internal cavity of the protein, into the solution, using both types of these pores as gates for migration. The Cip molecule was pulled along a certain vector using the parameter *pull-coord-geometry* = *direction*. The umbrella potential was used. The rate of change of the center of mass of Cip relative to center of mass of Dps was equal to 0.02 nm per ps. The harmonic force constant was 2000 kJ mol^{-1} nm^{-2}. For sterically less accessible regions of the protein, additional studies were carried out with parameters of 0.005 nm per ps and 500 kJ mol^{-1} nm^{-2} to obtain starting configurations from less favorable positions. From the resulting trajectory, 100 points (the centers of the umbrella sampling 'windows') were selected, uniformly distributing Cip along the axis, from the center of the protein to 4.5 Å from its surface. At each point, a trajectory of 20 ns duration was simulated (the constant of the confining harmonic potential was 1000 kJ mol^{-1} nm^{-2}). The free energy profile [Figure 2(*a*)] relative to the selected coordinate (mean force potential) was reconstructed using the weighted histogram analysis method, the standard error was estimated using 500 bootstraps. Simulations showed that, according to the free energy profile, it is advantageous for Cip molecules to penetrate from the ferritin pore into the cavity of the Dps protein ($\Delta\Delta G \approx -10$ kcal mol^{-1}). And through the pores of the Dps type, the antibiotic does not penetrate due to steric hindrances, as evidenced by the insufficient population of the Dps pore areas even when changing the umbrella simulation parameters. Based on the data obtained, it can be assumed that when exposed to high concentrations of Cip, the

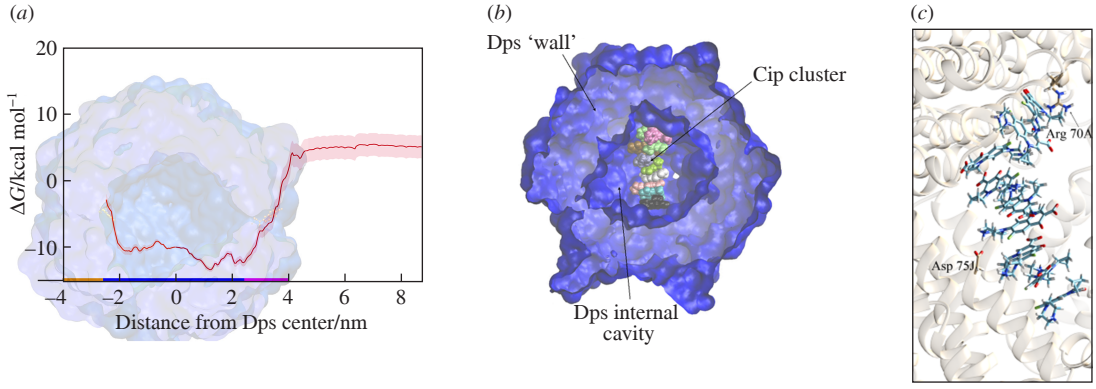

Figure 2 (*a*) Free energy profile along the axis passing through the center of the Dps dodecamer (corresponds to coordinate 0 on the abscissa). Colored areas on the abscissa correspond to the Dps pore (yellow), the internal cavity (blue) and the ferritin pore (pink). For clarity, a shaded Dps molecule is shown in the background of the figure. (*b*) Dps molecule 'in cross section': the internal cavity and the 'wall' of the protein are visible. Inside the protein there is a cluster of nine Cip molecules, colored in different colors. (*c*) Enlarged image of the Cip cluster interacting with Arg70 of chain A and Asp75 of chain J in Dps.

Dps protein can perform a protective function by capturing the antibiotic inside the globule.

Next, using classical molecular dynamics methods, the molecular mechanisms of interactions of several Cip molecules with the internal and external surfaces of the Dps protein and the DNA–Dps complex were investigated. The studies were carried out in the Gromacs package (all-atom force field AMBER99–PARMBSC1, SPC/E water model). The previously developed molecular dynamics protocol[13] included minimization of the potential energy by the steepest descent method, followed by relaxation of the system for 200 ps at constant volume and then pressure. During the simulation, the temperature of 301 K was maintained by a Langevin thermostat with a friction constant of 0.5 ps^{-1}, and the pressure of 1 atm was maintained by a Parrinello–Rahman barostat with a time constant of 2 ps. Long-range electrostatic interactions were calculated using the particle mesh Ewald summation method. The cutoff radii for all types of interactions were taken to be 1.5 nm. To search for a possible distribution of Cip molecules in the internal cavity of the protein, twelve Cip molecules were randomly placed inside a Dps molecule. During 0.1 μs simulations, they were separated into stable clusters. Figure 2(*b*),(*c*) shows an example of such clusters containing nine molecules. This suggests that Cip molecules may be tightly packed inside the protein. The clusters are held by the protein due to interactions with charged amino acid residues. Thus, in the example in Figure 2(*b*),(*c*), the positively charged nitrogen of Arg70 interacts with the oxygen of Cip, and the negatively charged oxygen of Asp75 interacts with the nitrogen of Cip. The Cip molecules are held together mainly by stacking interactions. The release of the antibiotic from the internal cavity of Dps can probably occur under conditions that promote the disintegration of Dps into subunits.

The molecular mechanisms of Cip interaction with Dps and the possible effect of Cip on the Dps complex with DNA in solution were assessed using the molecular dynamics protocol described above. A 25-base-pair DNA was used in the simulation.[12] The Cip distribution in the periodic box was set randomly. The processes of Cip adsorption on the Dps surface were observed over a time interval of 0.5 μs at a temperature of 301 K. Analysis of the molecular dynamics trajectory showed that at a time point of ~100 ns, single Cip molecules are adsorbed on the protein surface. Then, over a time interval of up to 250 ns, adsorption of Cip clusters occurs.

It turned out that the main Cip binding sites on the Dps protein surface are charged amino acid residues, including lysine residues. Most often, these are the Lys10 residues, which ensure protein binding to DNA, and Lys101. Cip can change the fine-tuning of DNA–Dps interactions. Thus, the dynamics in the presence of 50 Cip molecules per Dps molecule shows that half of the Dps N-termini are largely bound to Cip [Figure 3(*a*)], with the number of contacts exceeding 500. This leads to a change in the N-terminus dynamics, when key lysine amino acid residues are excluded from interaction with DNA by Cip molecules. As can be seen in Figure 3(*b*), Cip is distributed both on the Dps surface and between Dps and DNA. Figure 3(*c*) shows one of the Dps subunits (the others are hidden) and Cip molecules surrounding the key DNA-binding Lys10 residue. At the same time, the Cip molecules themselves are able to facilitate the binding of Dps to DNA, providing additional bridges between DNA and Dps.

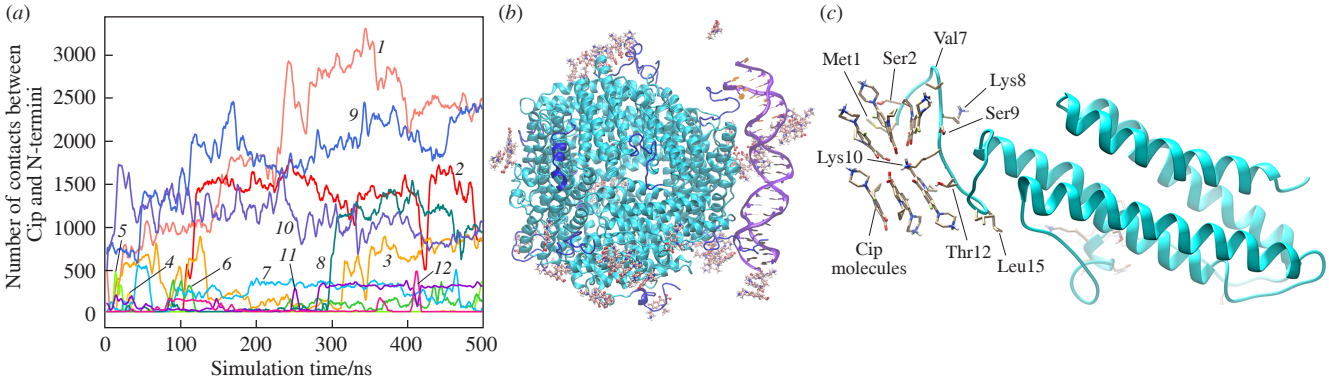

Figure 3 (*a*) Number of contacts between Cip atoms and the N-terminal atoms of Dps. The numbers next to the differently colored curves correspond to the ordinal numbers of Dps subunits, as listed in PDB ID: 6QVX. (*b*) Dps–DNA complex formed in 0.5 μs in the presence of Cip, in which the Dps protein is depicted as blue helices, the N-termini of all 12 Dps subunits are highlighted in blue, DNA is represented by a purple helix and Cip molecules are shown as ball-and-stick models in pink. (*c*) One of the Dps subunits (ice blue) in the Dps–DNA complex, N-terminus of which is surrounded by six Cip molecules. The main amino acid residues of the N-terminus interacting with Cip are labeled.

In this work, the interaction of Cip with the Dps protein, the main DNA-protective protein of the stationary phase of bacterial culture growth, was investigated. It was shown that the antibiotic Cip is adsorbed on the surface of the Dps protein, reducing the mobility of its N-termini and inserting itself between the protein and DNA molecules. This changes the fine-tuning of DNA–Dps interactions: Cip can block key amino acids of the N-termini (Lys10, *etc.*), but less stable protein–DNA connections arise *via* Cip clusters. Studies of the free energy of interaction between Cip and Dps using docking method show that the average binding affinity of Cip to the ferritin pores of Dps is $\Delta G \approx -6.9$ kcal mol^{-1}, while that to the areas of the internal cavity near the Dps pores and to the N-termini is $\Delta G \approx -6.7$ kcal mol^{-1}. The potential of mean force investigation shows that $\Delta\Delta G \approx -10$ kcal mol^{-1} between the ferritin pore and the internal cavity of Dps. This suggests that some part of the Cip molecules can penetrate the protein. The data on the effect of the antibiotic Cip on the Dps protein obtained by molecular modeling methods contribute to the elucidation of the mechanisms of bacterial resistance to antibiotics associated with the action of the Dps protein and will help in the development of new effective methods for the destruction (neutralization) of pathogenic microorganisms. Cip is an easily accessible and inexpensive antibacterial agent. Although bacterial resistance to antibiotics has been increasing recently, it is possible to combine the use of antibiotics with other antibacterial measures (UV, temperature, acid shock, *etc.*) to achieve the desired results in antibacterial control. This work is part of a larger effort to develop the best method for influencing bacteria. Understanding the molecular mechanisms of interaction between Cip and the main DNA-protective protein of the stationary phase of bacterial culture growth will allow the use of antibacterial agents in this growth phase in the future.

This work was financially supported by the Russian Science Foundation (grant no. 23-24-00250). The computations were performed on MVS-10P at the Joint Supercomputer Center of the Russian Academy of Sciences.

References

1 K. Orban and S. E. Finkel, *J. Bacteriol.*, 2022, **204**, e00036-22; https://doi.org/10.1128/jb.00036-22.
2 A. A. Talukder and A. Ishihama, *Adv. Microbiol.*, 2014, **4**, 1095; https://doi.org/10.4236/aim.2014.415120.
3 L. N. Calhoun and Y. M. Kwon, *J. Appl. Microbiol.*, 2011, **110**, 375; https://doi.org/10.1111/j.1365-2672.2010.04890.x.
4 N. Loiko, K. Tereshkina, V. Kovalenko, A. Moiseenko, E. Tereshkin, O. S. Sokolova and Y. Krupyanskii, *Biology*, 2023, **12**, 853; https://doi.org/10.3390/biology12060853.
5 E. Chiancone and P. Ceci, *Biochim. Biophys. Acta, Gen. Subj.*, 2010, **1800**, 798; https://doi.org/10.1016/j.bbagen.2010.01.013.
6 S. M. Williams and D. Chatterji, in *Macromolecular Protein Complexes III: Structure and Function*, eds. J. R. Harris and J. Marles-Wright, Springer, Cham, 2021, pp. 177–216; https://doi.org/10.1007/978-3-030-58971-4_3.
7 T. Lackraj, S. Birstonas, M. Kacori and D. Barnett Foster, *J. Bacteriol.*, 2020, **202**, e00114-20; https://doi.org/10.1128/JB.00114-20.
8 L. N. Calhoun and Y. M. Kwon, *Int. J. Antimicrob. Agents*, 2011, **37**, 261; https://doi.org/10.1016/j.ijantimicag.2010.11.034.
9 M. A. Ozma, E. Khodadadi, M. A. Rezaee, M. Asgharzadeh, M. Aghazadeh, E. Zeinalzadeh, K. Ganbarov and H. S. Kafil, *Curr. Pharm. Biotechnol.*, 2022, **23**, 1245; https://doi.org/10.2174/1389201022666210908153234.
10 I. V. Polyakov, M. G. Khrenova, B. L. Grigorenko and A. V. Nemukhin, *Mendeleev Commun.*, 2022, **32**, 739; https://doi.org/10.1016/j.mencom.2022.11.010.
11 V. V. Abzianidze, V. V. Kadochnikov, D. S. Suponina, N. V. Skvortsov, P. P. Beltyukov, V. N. Babakov, D. V. Krivorotov, E. M. Barysheva and A. V. Garabadzhiu, *Mendeleev Commun.*, 2023, **33**, 534; https://doi.org/10.1016/j.mencom.2023.06.030.
12 N. G. Loiko, E. V. Tereshkin, V. V. Kovalenko, Y. F. Krupyanskii and K. B. Tereshkina, *Microbiology*, 2023, **92**, S78; https://doi.org/10.1134/S0026261723603640.
13 E. V. Tereshkin, N. G. Loiko, K. B. Tereshkina, V. V. Kovalenko and Y. F. Krupyanskii, *Russ. J. Phys. Chem. B*, 2022, **16**, 726; https://doi.org/10.1134/S1990793122040285.
14 F. N. Novikov and G. G. Chilov, *Mendeleev Commun.*, 2009, **19**, 237; https://doi.org/10.1016/j.mencom.2009.09.001.
15 A. M. Kulakova and M. G. Khrenova, *Mendeleev Commun*., 2021, **31**, 185; https://doi.org/10.1016/j.mencom.2021.03.013.
16 A. M. Toikka and A. V. Petrov, *Mendeleev Commun.*, 2023, **33**, 413; https://doi.org/10.1016/j.mencom.2023.04.036.
17 A. Shariati, M. Arshadi, M. A. Khosrojerdi, M. Abedinzadeh, M. Ganjalishahi, A. Maleki, M. Heidary and S. Khoshnood, *Frontiers in Public Health*, 2022, **10**, 1025633; https://doi.org/10.3389/fpubh.2022.1025633.
18 K. E. Knoll, Z. Lindeque, A. A. Adeniji, C. B. Oosthuizen, N. Lall and D. T. Loots, *Microorganisms*, 2021, **9**, 1158; https://doi.org/10.3390/microorganisms9061158.
19 N. Ojkic, E. Lilja, S. Direito, A. Dawson, R. J. Allen and B. Waclaw, *Antimicrob. Agents Chemother.*, 2020, **64**, e02487-19; https://doi.org/10.1128/AAC.02487-19.
20 W. Tian, C. Chen, X. Lei, J. Zhao and J. Liang, *Nucleic Acids Res.*, 2018, **46**, W363; https://doi.org/10.1093/nar/gky473.

Received: 8th July 2024; Com. 24/7567